

◀试验研究▶

# 操作参数对柱形旋流器油水分离性能的影响\*

史仕荧<sup>1</sup> 邓晓辉<sup>2</sup> 吴应湘<sup>1</sup> 马乃庆<sup>1</sup>

(1. 中国科学院力学研究所 2. 中海油深圳分公司)

**摘要** 为了判断柱形旋流器的结构设计是否满足实际生产需要,从操作参数的角度研究了油水混合物流速和分流比对柱形旋流器油水分离性能的影响。基于柱形旋流器内部的流动特征,分析了油滴分离的临界条件,得到了油滴从溢流口流出的临界粒径计算公式。分析结果认为,随主管路中油水混合物流速的增加,从溢流口流出的累积油相体积先增大后减小;在溢流口流量一定的前提下,溢流口含油体积分数先增大后减小,理论分析与试验得到的结果一致。

**关键词** 柱形旋流器 油水分离 混合物流速 分流比 操作参数

## 0 引言

柱形旋流器是一种新型的油水分离设备,目前对其研究还处于初级阶段。研究柱形旋流器油水分离性能的文献较少。Listewnik J<sup>[1]</sup>研究了4个入口结构的柱形旋流器油水分离效率; Seyda B<sup>[2]</sup>对小直径柱形旋流器中的油水分离进行了数值模拟; Oropeza - Vazquez C<sup>[3]</sup>对不同入口流型和油滴粒径分布进行了相关试验;文献[4]研究了不同油水表观流速对柱形旋流器油水分离的影响。调研发现,目前关于不同油水混合物的流速、分流比对柱形旋流器油水分离性能影响的文献有限。对于油田在某一段时间来说,采出液含油体积分数和流量较稳定,如何判断柱形旋流器的结构设计是否满足实际生产需要,即给出一定结构的柱形旋流器最佳操作区间,成为结构设计者首先要考虑的问题。为此,笔者将从操作参数的角度,研究油水混合物流速和分流比对柱形旋流器油水分离性能的影响,以期对柱形旋流器的结构设计提供参考。

## 1 试验研究

### 1.1 试验流程

试验中分离介质为 LP-14 白油和水。物性参

数为:  $\rho_o = 836.0 \text{ kg/m}^3$ 、 $\mu_o = 0.031 \text{ kg/(m}\cdot\text{s)}$ 、 $\rho_w = 998.0 \text{ kg/m}^3$ 、 $\mu_w = 0.001 \text{ kg/(m}\cdot\text{s)}$ 。

试验工艺流程见图1。油、水分别在油泵和水泵的增压作用下,流经流量计量装置,通过Y形管混合后进入柱形旋流器入口,在柱形旋流器中进行分离,之后对流经上部溢流口的流体进行取样并测定含油体积分数,流经底流口的流体则流回油水混合罐进行重力沉降分离,分离后的油、水各自流回油箱、水箱。

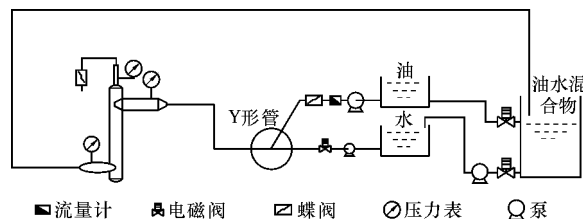


图1 试验工艺流程示意图

### 1.2 柱形旋流器结构设计

柱形旋流器结构简图如图2所示。入口水平圆管与竖直柱形管通过一段喷嘴状的渐变管切向相接,并使渐变管段2端的面积之比为10:1,使流体进入柱体的切向速度变为渐变管段前速度的10倍,随后油水混合物在柱体中形成旋流场,油、水因密度的不同在径向上沉降分离,油滴运动到轴心形成油核从溢流口流出,水运动到器壁并从底流口

\* 基金项目: 国家科技重大专项“大型油气田及煤层气开发”子课题“海相礁灰岩稠油油藏(特)高含水期精细开发技术研究”(2008ZX05024-004-010)。

排出。

### 1.3 试验步骤

(1) 向水箱和油箱内加注清水和油。

(2) 打开油泵和水泵, 调节流量, 改变入口油水的表观流速, 从而改变柱形旋流器入口的含油体积分数, 并记录油、水流量。

(3) 溢流口流量通过溢流口处的阀门来控制, 待旋流器内部形成稳定的油核后, 在溢流口处计时采样, 记录采样中油、水的体积分数及采样时间。

(4) 根据记录的数据换算出柱形旋流器的入口含油体积分数、分流比及溢流口含油体积分数。

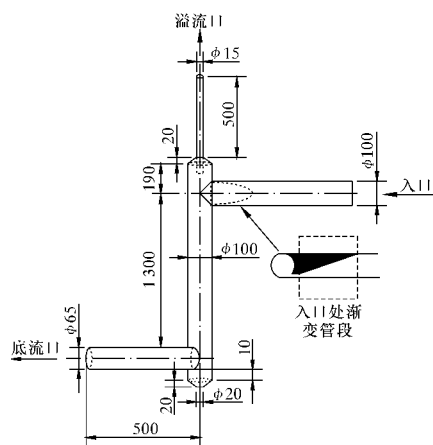


图2 柱形旋流器结构简图

## 2 试验结果分析

### 2.1 分流比对溢流口含油体积分数的影响

在入口油水混合流速为  $0.91 \text{ m/s}$ 、含油体积分数为  $3\%$  时, 柱形旋流器溢流口含油体积分数随分流比的变化规律如图3所示。从图可以看出, 溢流口的含油体积分数随分流比的增加先增大后减小, 当分流比达到  $0.15$  时, 溢流口含油体积分数

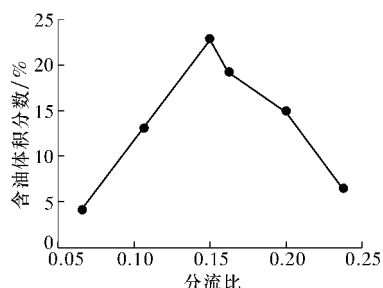


图3 溢流口含油体积分数随分流比的变化规律

达到最大值  $23\%$ ; 当分流比为  $0.07$  和  $0.24$  时, 溢流口含油体积分数均在  $5\%$  左右。柱形旋流器存在最优分流比。当分流比较小时, 由于总是存在沿壁面运动到溢流口的短路流部分 (水分含量较多), 使得油相所占的比例减小, 故溢流口含油体积分数

相对较小; 当分流比逐渐增大时, 大部分油核从溢流口流出, 故含油体积分数增大; 当分流比进一步增加时, 由于单位时间内进入旋流器中的油有限, 增多的那部分流量最终由水来补充, 故含油体积分数又减小。

### 2.2 入口流速对溢流口含油体积分数的影响

入口含油体积分数为  $3\%$ , 分流比为  $0.24$  时, 溢流口含油体积分数随入口混合流速的变化曲线如图4所示。从图中可以看出, 随着入口流速的增加, 溢流口含油体积分数先增大后减小, 当混合流速在  $0.55 \text{ m/s}$  时, 溢流口含油体积分数达到最大值, 为  $14\%$ , 当流速较小或较大时, 溢流口含油体积分数均低于此值。说明柱形旋流器存在最佳入口流速。

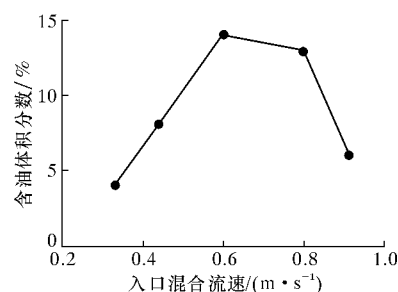


图4 溢流口含油体积分数随入口混合流速的变化曲线

上述规律可以用油滴在旋流器中的运动来说明, 油水在旋流器中的流动从二维平面来看, 属于组合螺旋流 (自由涡和强制涡) 运动。油水的分离过程主要在自由涡区域完成, 即假设油滴运动到强制涡区域就可以从溢流口流出。在上述前提下, 建立油滴在柱形旋流器中的分离模型, 并做如下假设: ①柱形旋流器中的强制涡区域是以溢流口圆截面为底面、向柱体内部延伸的柱体; ②油滴在切向入口与柱体强制涡区域之间的环形区域中下行速度与水平速度相同; ③初入柱形旋流器中的流体切向速度等于入口速度; ④油滴的径向沉降服从 Stokes 定律; ⑤油滴为刚性小球。

液滴进入强制涡区域进而从溢流口流出的条件为: 液滴从入口处运动到强制涡区域柱体下端面所需的时间  $t_1 \geq$  液滴从壁面  $D_H/2$  处沉降到  $D_o/2$  处的沉降时间  $t_2$ 。

#### (1) $t_1$ 的计算

由假设②和③可知,  $t_1$  由柱体壁面与柱体强制涡区域之间的环形区域体积和入口流量决定, 即

$$t_1 = \frac{\frac{\pi}{4}(D_H^2 - D_o^2) \frac{H}{2}}{\frac{\pi}{4} D_m^2 U_m} = \frac{(D_H^2 - D_o^2) H}{2 D_m^2 U_m} \quad (1)$$

式中  $D_H$ ——柱形旋流器柱体直径, m;  
 $D_o$ ——溢流管直径, m;  
 $D_m$ ——主管路直径, m;  
 $H$ ——柱体的高度, m;  
 $U_m$ ——主管路中的混合流速, m/s。

(2)  $t_2$  计算

根据假设④, 由 Stocks 沉降速度公式得:

$$\frac{dr}{dt} = U_r = \frac{d^2(\rho_w - \rho_o) U_t^2}{18\mu r} \quad (2)$$

式中  $r$ ——液滴所在位置的半径, m;  
 $d$ ——液滴的粒径, m;  
 $U_t$ ——液滴切向速度, m/s;  
 $\mu$ ——水的粘度, Pa·s;  
 $t$ ——时间, s。

在自由涡区域, 液滴切向速度的表达式为:

$$U_t r^n = C = \alpha U_{in} \left(\frac{D_H}{2}\right)^n \quad (3)$$

式中  $n$ 、 $C$ ——常数,  $n$  在 0.5 ~ 0.9 之间;  
 $\alpha$ ——速度衰减系数,  $\alpha = 0 \sim 1$ ;  
 $U_{in}$ ——旋流器入口与柱体相接处的流速, m/s。

将式 (3) 代入式 (2) 并分离变量积分 (积分上、下限由油滴沉降时的时间位置对应关系确定: 即  $t = 0$  时, 油滴在  $D_H/2$  处,  $t = t_2$  时, 油滴在  $D_o/2$  处) 得沉降时间  $t_2$ :

$$t_2 = \frac{9\mu \left[ \left(\frac{D_H}{2}\right)^{2n+2} - \left(\frac{D_o}{2}\right)^{2n+2} \right]}{(n+1) d^2 (\rho_w - \rho_o) \alpha^2 U_{in}^2 \left(\frac{D_H}{2}\right)^{2n}} \quad (4)$$

由  $t_1 \geq t_2$  得粒径的表达式:

$$d \geq \left\{ \frac{18D_m^2 \mu \left[ \left(\frac{D_H}{2}\right)^{2n+2} - \left(\frac{D_o}{2}\right)^{2n+2} \right] U_m}{(n+1) (\rho_w - \rho_o) \alpha^2 U_{in}^2 \left(\frac{D_H}{2}\right)^{2n} (D_H^2 - D_o^2) H} \right\}^{\frac{1}{2}} \quad (5)$$

$d$  取最小值, 即为油滴能被分离的最小粒径。

柱形旋流器入口前的主管路直径为 50 mm, 入口管段变截面前的管径为 100 mm, 变截面的面积为入口管段变截面前面积的  $\frac{1}{4}$ , 则由流量守恒原理可得:

$$U_{in} = \frac{5}{2} U_m \quad (6)$$

将式 (6) 代入式 (5), 并考虑等式成立的临界条件, 得油滴能被分离的临界粒径表达式为:

$$d_{pc} = \left\{ \frac{72D_m^2 \mu \left[ \left(\frac{D_H}{2}\right)^{2n+2} - \left(\frac{D_o}{2}\right)^{2n+2} \right]}{25(n+1) (\rho_w - \rho_o) \alpha^2 U_m \left(\frac{D_H}{2}\right)^{2n} (D_H^2 - D_o^2) H} \right\}^{\frac{1}{2}} \quad (7)$$

李雪斌等<sup>[5]</sup> 分析了旋流器中液滴聚结机理, 发现对于特定的旋流器和分离物料, 存在临界流量, 当入口流量小于临界流量时, 分散相液滴的最大粒径随入口流量的增加而增大; 当入口流量大于临界流量时, 分散相液滴的最大粒径随入口流量的增加而减小。临界流量的表达式为:

$$Q_{pc} = \left( \frac{3 \cdot 19 D_H^{3/2} V^{2/3}}{K^{2/3} \rho_w^{3/2}} \right)^{1/(m+1.2)} = \frac{\pi}{4} D_m^2 U_{pc} \quad (8)$$

式中  $Q_{pc}$ ——临界入口流量,  $m^3/s$ ;  
 $V$ ——旋流器体积,  $m^3$ ;  
 $K$ 、 $m$ ——系数, 由试验获得;  
 $U_{pc}$ ——对应的临界主管路混合流速, m/s。

分散相液滴的最大粒径与入口流量之间的关系

如下:

当  $Q \leq Q_{pc}$  时

$$d_{od \max} = KQ^m = K \left( \frac{\pi}{4} D_m^2 U_m \right)^m \quad (9)$$

当  $Q > Q_{pc}$  时

$$d_{od \max} = \frac{3 \cdot 19 D_H^{1.6} V^{0.4} \sigma^{0.6}}{K^{0.4} \rho_w^{0.6} Q^{1.2}} = \frac{4 \cdot 27 D_H^{1.6} V^{0.4} \sigma^{0.6}}{K^{0.4} \rho_w^{0.6} D_m^{2.4} U_m^{1.2}} \quad (10)$$

式中  $\sigma$ ——油水界面张力, N/m;

$d_{od \max}$ ——油滴的最大粒径。

Crowe C T<sup>[6]</sup> 和 Karabelas A J<sup>[7]</sup> 基于 Rosin-Rammler 粒径分布得出体积分数表达式, 将小于等于最大粒径  $d_{od \max}$  的体积分数设为 0.999, 笔者采用与文献 [3] 相同的设置, 得到粒径在  $d_{pc} \sim d_{od \max}$  之间的体积分数表达式为:

$$V_{cum} = \exp \left[ -6.9077 \left( \frac{d_{pc}}{d_{od \max}} \right)^{2.6} \right] \quad (11)$$

当  $Q \leq Q_{pc}$  时, 可得:

$$\frac{d_{pc}}{d_{od \max}} = U_m^{-0.5-m} \times \left\{ \frac{72D_m^2 \mu \left[ \left(\frac{D_H}{2}\right)^{2n+2} - \left(\frac{D_o}{2}\right)^{2n+2} \right]}{25(n+1) (\rho_w - \rho_o) \alpha^2 \left(\frac{D_H}{2}\right)^{2n} (D_H^2 - D_o^2) H} \right\}^{\frac{1}{2}} \div \left[ K \left( \frac{\pi}{4} D_m^2 \right)^m \right] \quad (12)$$

当  $Q > Q_{pc}$  时, 可得:

$$\frac{d_{pc}}{d_{od,max}} = 0.234 U_m^{0.7} K^{0.4} \rho_w^{0.6} D_m^{2.4} \times \left\{ \frac{72 D_m^2 \mu \left[ \left( \frac{D_H}{2} \right)^{2n+2} - \left( \frac{D_o}{2} \right)^{2n+2} \right]}{25(n+1)(\rho_w - \rho_o) \alpha^2 \left( \frac{D_H}{2} \right)^{2n} (D_H^2 - D_o^2) H} \right\}^{\frac{1}{2}} \div \left( D_H^{1.6} V^{0.4} \sigma^{0.6} \right) \quad (13)$$

由式(12)、式(13)可知, 对于特定的旋流器和分离物料,  $d_{pc}/d_{od,max}$  是  $U_m$  的单值函数, 并随  $U_m$  的增大先减小后增大, 而  $V_{cum}$  随  $d_{pc}/d_{od,max}$  的增大而减小, 故随着  $U_m$  的增大,  $V_{cum}$  先增大后减小。

因此, 在入口含油体积分数和溢流口流量一定的前提下, 溢流口含油体积分数先增大后减小。

### 2.3 流速对最佳分流比区间的影响

图5显示了在入口含油体积分数为3%时, 溢流口含油体积分数随混合流速、分流比变化的分布。由图可见, 在油水混合流速一定的条件下, 溢流口含油体积分数随分流比的变化规律与2.1节相似, 都存在一个峰值, 与峰值对应的即为最优分流比。同时随着油水混合流速的增大, 最优分流比所处的区间向左移动, 即最优分流比的数值随油水混合流速的增大而减小, 且随着速度的增大, 最大溢流口含油体积分数先增大后减小。这说明对于柱形旋流器结构, 在特定的入口含油体积分数下, 存在最佳工况, 可使旋流器的分离性能达到最佳。

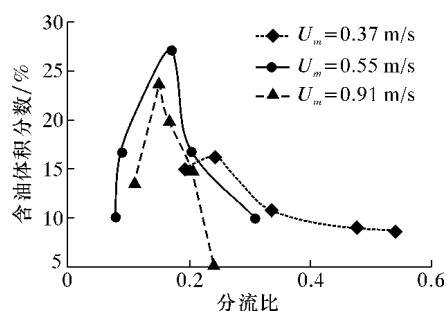


图5 溢流口含油体积分数随混合流速、分流比变化的分布图

## 3 结 论

(1) 分流比是影响柱形旋流器油水分离性能的一个主要因素, 在油水混合流速和含油体积分数一定的条件下, 溢流口含油体积分数随分流比的增加先增大后减小。

(2) 油水混合物在主管路中的流速是影响柱

形旋流器油水分离性能的另一个主要因素。当保持油水在柱形旋流器入口的含油体积分数、溢流口分流比一定时, 随着油水混合物流速的增加, 溢流口含油体积分数先增大后减小。这表明, 对于结构一定的柱形旋流器存在最佳油水处理量, 此时溢流口含油体积分数最大。

(3) 基于柱形旋流器内部流动特征, 分析了油滴分离的临界条件, 得到了油滴从溢流口流出的临界粒径计算公式, 结合前人在液滴聚并破碎方面的研究成果发现, 随主管路中混合物流速的增加, 从溢流口流出的累积油相体积先增大后减小; 在溢流口流量一定的前提下, 溢流口含油体积分数先增大后减小, 理论分析与试验得到的结果一致。

### 参 考 文 献

- [1] Listewnik J. Some factors influencing the performance of de-oiling hydrocyclones for marine applications [C] // Second International Conference on Hydrocyclones, England, 1984: 19-21.
- [2] Seyda B. Separation of a light dispersion in a cylindrical vortex chamber [R]. Michigan State University, 1991.
- [3] Oropeza-Vazquez C, Afanador E, Gomez L, et al. Oil-water separation in a novel liquid-liquid cylindrical cyclone (LLCC) compact separator - experiments and modeling [J]. *Journals of Fluids Engineering*, 2004, 126(7): 553-564.
- [4] Oropeza-Vazquez C. Multiphase flow separation in liquid-liquid cylindrical cyclone and gas-liquid-liquid cylindrical cyclone compact separators [D]. Tulsa: The University of Tulsa, 2001.
- [5] 李雪斌, 袁惠新. 旋流器内液滴聚结机理的研究 [J]. *矿山机械*, 2006, 34(7): 67-69.
- [6] Crowe C T, Sommerfeld M, Tsuji Y. *Multiphase flows with droplets and particles* [C]. CRC press, Boca Raton, FL, 1998.
- [7] Karabelas A J. Droplet size spectra generated in turbulent pipe flow of dilute liquid-liquid dispersions [J]. *AIChE J*, 1978, 24(2): 170-180.

第一作者简介: 史仕英, 女, 生于1984年, 2007年毕业于武汉理工大学能源与动力工程学院, 现为中国科学院力学研究所在读博士研究生, 从事管道式油水分离器的研究工作。地址: (100190)北京市海淀区。电话: (010)82544173。E-mail: shishiying123@163.com。

收稿日期: 2010-11-25

(本文编辑 王刚庆)

## ABSTRACTS OF SELECTED ARTICLES

Zhang Haiping(*Research Institute of Petroleum Engineering Technology, SINOPEC, Beijing*), Suo Zhongwei, Tao Xinghua. **The structural design and experimental study of the jet-type hydro-hammer.** *CPM*, 2011, 39(7): 1-3

The welding and bonding position of the jet-type hydro-hammer used by rotary percussion drilling is liable to cracking. As a result, there appear leakage, pressure relief and failure to establish the operating pressure of the upper and lower cavities of the cylinder, leading to hammer shutdown or its unstable operation or adverse effect on its performance. Therefore, the integrated structure of the hammer cylinder was designed, carefully choosing special high hot-work die steel material (HHD), adopting monoblock casting in its shaping and adopting wet nitriding and oxidation to process the cylinder surface. The laboratory performance experiment and field application test of the hammer with this structure were carried out. The result indicated that the performance of the hammer was improved, with desirable operating stability and parametric adjustability. It can effectively improve the penetration rate of the deep hard rock formation, prevent hole deviation and reduce drilling costs.

**Key words:** rotary percussion drilling, jet-type hydro-hammer, wall attachment effect, integrated casting cylinder, penetration rate

Shi Shiyong(*Institute of Mechanics, Chinese Academy of Sciences, Beijing*), Deng Xiaohui, Wu Yingxiang, et al. **The effect of operating parameters on the oil-water separation performance of the cylindrical cyclone.** *CPM*, 2011, 39(7): 4-7

To make a judgement of whether the structural design of cylindrical cyclone meets the needs of practical production, the effect of the velocity and shunt ratio of the mixture on the oil-water separation performance of the cylindrical cyclone was studied from the perspective of operating parameters. Based on the flow characteristics of the cyclone, the critical condition for oil droplet separation was analyzed and the critical particle diameter calculation formula for oil droplets to flow from the overflow outlet was obtained. The result indicated that, with the increase of the mixture velocity in the main pipeline, the cumulative oil phase volume from the overflow outlet increased first and then decreased. In the precondition that the flowrate at the overflow outlet was fixed, the oil content of the overflow outlet increased first and then decreased. The theoretical analysis was in agreement with the result obtained.

**Key words:** cylindrical cyclone, oil-water separation, mixture velocity, shunt ratio, operating parameter

Wang Zhiming(*Department of Oilfield Technology Affairs, China Oilfield Services Limited, Beijing*), Guo Yun, Shang Jie. **The design and experimental study of the hybrid excitation downhole turbogenerator.** *CPM*, 2011, 39(7): 8-10, 14

In light of the low power and poor high temperature resistance of existing downhole generators, a kind of hybrid

excitation generator was designed. The design scheme and calculation procedure of the generator were formulated. The effect of high temperature environment on the turbogenerator and the measures to be taken were analyzed. The effect of the guide wheel and the turbine type on the power generation was also discussed. Through the experiment the relationship between high temperature, high pressure, drilling pump displacement and the performance of the turbogenerator was studied. The result indicated that high pressure had no effect on the output power of the generator. The efficiency decreased remarkably with the increase of temperature. In laboratory conditions the power of the generator could meet the needs of system power supply.

**Key words:** measurement while drilling, hybrid excitation, downhole turbogenerator, guide wheel, turbine

He Xia(*College of Mechanical and Electrical Engineering, Southwest Petroleum University, Chengdu*), Wang Degui, Liu Qingyou, et al. **A simulation analysis of the rock-breaking mechanism of the air hammer bit.** *CPM*, 2011, 39(7): 15-18

Based on the nonlinear kinetic theory, the ANSYS/LS DYNA explicit kinetic analysis software was adopted to establish the simulation model of air hammer bit and rock-breaking mechanism. The simulation analysis of the rock-breaking process of the bit was conducted. It was thought that the rock-breaking process included four stages, namely, elastic deformation stage, plastic deformation stage, crack initiation stage and fragmentation completion stage. Finally, a comparison was conducted of the rock-breaking result of granite, sandstone, dolomite, shale and limestone under the same condition. The result showed that the granite invasion depth was minimum and that of limestone was maximum. The volume crushing of shale was minimum and that of granite was maximum. The simulation found that the rock volume fracture took place at the unloading stage. Although the volume crushing and invasion depth of different types of rocks were different, the overall tendency of rock-breaking curve remained the same. In other words the rock-breaking law was similar.

**Key words:** air hammer bit, rock-breaking mechanism, simulation model, ANSYS

Yu Jie(*Research Institute of Oil Production Technology, Xinjiang Oilfield Company, Urumqi*), Pan Jingjun, Cai Gang, et al. **The research and application of electric ignition technology in Hongqian well area of Xinjiang Oilfield.** *CPM*, 2011, 39(7): 19-21

The key to the success of heavy oil fireflooding is reservoir ignition. To improve the success rate of ignition, electric ignition was adopted from the angle of safety and practicality. The downhole electric heater, its ignition technology string and the monitoring system for ignition process were developed. The heater was installed with several thermometric sensors. It could achieve the offline simulation monitoring and online monitoring of the distribution and